EClinicalMedicine 24 (2020) 100434

Contents lists available at ScienceDirect

EClinicalMedicine

journal homepage: https://www.journals.elsevier.com/eclinicalmedicine

Research Paper

Megakaryocytes and platelet-fibrin thrombi characterize multi-organ thrombosis at autopsy in COVID-19: A case series

Amy V. Rapkiewicz[a,*], Xingchen Mai[b], Steven E. Carsons[a], Stefania Pittaluga[c], David E. Kleiner[c], Jeffrey S. Berger[b], Sarun Thomas[a], Nicole M. Adler[b], David M. Charytan[b], Billel Gasmi[c], Judith S. Hochman[b], Harmony R. Reynolds[b]

[a] NYU Winthrop Hospital, Chair and Autopsy Director, Department of Pathology, Long Island School of Medicine, 222 Station Plaza North, Suite 618, Mineola, NY, 11501, United States
[b] New York University Grossman School of Medicine, New York, NY, United States
[c] Center for Cancer Research, National Cancer Institute, National Institutes of Health, Bethesda, MD, United States

ARTICLE INFO

Article History:
Received 5 June 2020
Revised 8 June 2020
Accepted 9 June 2020
Available online 25 June 2020

Keywords:
"COVID-19"
"Autopsy"
"Megakaryocyte"
"Thrombosis"

ABSTRACT

Background: There is increasing recognition of a prothrombotic state in COVID-19. Post-mortem examination can provide important mechanistic insights.
Methods: We present a COVID-19 autopsy series including findings in lungs, heart, kidneys, liver, and bone, from a New York academic medical center.
Findings: In seven patients (four female), regardless of anticoagulation status, all autopsies demonstrated platelet-rich thrombi in the pulmonary, hepatic, renal, and cardiac microvasculature. Megakaryocytes were seen in higher than usual numbers in the lungs and heart. Two cases had thrombi in the large pulmonary arteries, where casts conformed to the anatomic location. Thrombi in the IVC were not found, but the deep leg veins were not dissected. Two cases had cardiac venous thrombosis with one case exhibiting septal myocardial infarction associated with intramyocardial venous thrombosis, without atherosclerosis. One case had focal acute lymphocyte-predominant inflammation in the myocardium with no virions found in cardiomyocytes. Otherwise, cardiac histopathological changes were limited to minimal epicardial inflammation ($n = 1$), early ischemic injury ($n = 3$), and mural fibrin thrombi ($n = 2$). Platelet-rich peri-tubular fibrin microthrombi were a prominent renal feature. Acute tubular necrosis, and red blood cell and granular casts were seen in multiple cases. Significant glomerular pathology was notably absent. Numerous platelet-fibrin microthrombi were identified in hepatic sinusoids. All lungs exhibited diffuse alveolar damage (DAD) with a spectrum of exudative and proliferative phases including hyaline membranes, and pneumocyte hyperplasia, with viral inclusions in epithelial cells and macrophages. Three cases had superimposed acute bronchopneumonia, focally necrotizing.
Interpretation: In this series of seven COVID-19 autopsies, thrombosis was a prominent feature in multiple organs, in some cases despite full anticoagulation and regardless of timing of the disease course, suggesting that thrombosis plays a role very early in the disease process. The finding of megakaryocytes and platelet-rich thrombi in the lungs, heart and kidneys suggests a role in thrombosis.
Funding: None.

1. Introduction

Severe acute respiratory syndrome coronavirus 2 (SARS-CoV-2) is responsible for the global pandemic of coronavirus disease 2019 (COVID-19). While the majority of patients with COVID-19 experience mild symptoms, serious complications including ARDS, hemodynamic shock, acute kidney injury, cardiac injury, and arrhythmia contribute to the high mortality rate [1]. Elevation of cardiac troponin is common in COVID-19 and has been associated with poorer outcomes [2–4]. ST-segment elevation myocardial infarction in a small series of patients with COVID-19 was associated with a relatively low likelihood of severe coronary artery disease (CAD) [5]. Myocardial injury in COVID-19 has been postulated to be due to viral myocarditis, but there has been a paucity of histologic evidence to determine the causes of troponin elevation.

There is growing recognition of an increased rate of thrombotic complications in patients with COVID-19, higher than in respiratory failure due to influenza, and with the notable observation that pulmonary thrombosis in the absence of lower extremity deep venous

* Corresponding author.
E-mail address: Rapkia01@nyumc.org (A.V. Rapkiewicz).

https://doi.org/10.1016/j.eclinm.2020.100434

Research in context

Evidence before this study

COVID-19 is associated with increased risk of thrombotic events. Previous pathology studies, identified by searching PubMed on June 7, 2020 for the terms "COVID-19″ and "autopsy" or "histopathology", have reported findings in multiple organs, including thrombi on gross inspection, but did not use special stains to identify megakaryocytes and platelets in tissues of patients dying with COVID-19. The presence of circulating megakaryocytes on autopsy in various organs was also researched, for which we searched PubMed on June 7, 2020 for "pathology" or "autopsy" and "megakaryocytes".

Added value of this study

We present a COVID-19 autopsy series including findings in lungs, heart, kidneys, liver, and bone, from a New York academic medical center. Regardless of anticoagulation status, all autopsies demonstrated platelet-rich thrombi in the pulmonary, hepatic, renal, and cardiac microvasculature. Megakaryocytes were seen in the vascular beds of multiple organs, and in higher than usual numbers in lungs and heart. Megakaryocyte numbers were increased as compared with patients who died of acute respiratory distress syndrome (ARDS) unrelated to COVID-19. We report two cases with myocardial venous thrombosis and troponin elevation, one of which exhibited myocardial infarction on gross inspection, illustrating a previously unrecognized mechanism of MI.

Implications of all available evidence

Thrombosis is an important contributor to pathologic mechanisms underpinning multi-organ failure, severe hypoxia and death in patients with COVID-19. Myocardial infarction may be caused by venous thrombosis in the absence of significant coronary artery atherosclerotic disease. Platelets and circulating megakaryocytes are likely to play an important role in the increased thrombotic risk associated with COVID-19.

thrombosis is frequently observed [6–9]. Autopsy series have demonstrated a high prevalence of microthrombi in pulmonary capillaries as well as pulmonary arterial thrombosis [10–12]. In biopsy samples obtained from skin and kidney, there were frequent microthrombi in the microvasculature [11,13]. In addition, autopsy reports have shown thrombus formation in less common areas, including the hepatic portal vein, the prostatic venous plexus and in the heart [10–12]. Observational studies suggest that anticoagulation therapy, including more intensive anticoagulation, may be associated with better outcomes in patients infected with COVID-19 [14,15].

The mechanism for this prothrombotic milieu is yet to be determined. We present results of the first seven autopsies from an academic New York medical center, including findings from lungs, hearts, kidneys, liver, and bone. We hypothesized that post-mortem examination would improve our understanding of the reasons for multi-organ failure and thrombosis in COVID-19.

2. Methods

Hospital-based autopsies were performed by Amy Rapkiewicz using personal protective equipment in a negative pressure facility with limited staff participating to reduce risk. Consecutive autopsies performed at NYU Winthrop Hospital among persons with laboratory-confirmed COVID-19 or who were under investigation and tested positive on post-mortem PCR were included. The lungs, heart, kidneys, spleen, lymph nodes, liver, bone, and skeletal muscle were evaluated in detail in all cases. Tissues were fixed in 10% buffered formalin for 72 h and routinely processed. Hematoxylin and eosin (H&E)-stained sections were prepared. Immunohistochemistry (IHC) was performed via epitope retrieval using Roche Benchmark Ultra with incubation time 16–32 min, depending on antibody. Sections were incubated with CD61 (Cell Marque, clone 2F2), CD20 (Predilute-Roche, clone L62), CD3 (Predilute- Roche, clone 2GV6), CD4 (Predilute-Roche, clone SP35), CD8 (Predilute-Roche, clone SP57) and a rabbit polyclonal anti-SARS nucleo-capsid protein antibody (Novus Biologicals) detection was carried out using OptiView DAB IHC kit.

For electron microscopy, tissue samples were fixed in 4% glutaraldehyde buffered in 0·1 M sodium cacodylate buffer, pH 7.5, washed in sodium cacodylate buffer, post-fixed in buffered 1% osmium tetroxide, en-bloc stained with a saturated solution of uranyl acetate in 40% ethanol, dehydrated in a graded series of ethanol, infiltrated in propylene oxide with Epon epoxy resin (LX112, Ladd industries, Burlington, VT), and embedded. Blocks were sectioned with a Reichert Ultracut microtome at 70 nm. The resulting grids were post-stained with 1% aqueous uranyl acetate followed by 0·5% aqueous lead citrate and scoped on a Zeiss EM 900 transmission electron microscope retro-fitted with an L3C digital camera (SIA, Duluth, GA). Electron microscopy was performed on limited samples based on resource availability, focusing on organs that were grossly abnormal, including lung (four cases), heart (four cases), kidney (five cases), liver (one case), fat (two cases), skeletal muscle (two cases), and bone marrow (one case).

Paraffin-embedded blocks of all tissues in all cases were sent to the Laboratory of Pathology of the National Cancer Institute for immunohistochemical consultation.

We counted numbers of megakaryocytes in the lungs and the hearts of 7 COVID-19 cases and, for comparison, 9 cases of patients who died with ARDS of other causes, selected as a convenience sample from autopsies previously performed at the National Cancer Institute between 2017 and 2020. In the lungs ten consecutive high-power fields (HPF, 40x magnification) were scored three times for each case, while the whole section of the heart was used to count megakaryocytes. Student's *t*-test was used to compare the number of megakaryocytes between COVID-19 and other ARDS cases. P values $<0{\cdot}05$ were considered statistically significant.

Chart review was performed to identify medical history, laboratory values (initial and peak, where available), and to review electrocardiography and imaging, when available.

Dr. Rapkiewicz had access to all data. Drs. Rapkiewicz and Reynolds had final responsibility for the decision to submit the manuscript.

Role of Funding: There was no external funding for this analysis. This study was supported, in part, by the Intramural Research Program of the NIH, National Cancer Institute.

Ethics: Reporting of this series of clinically indicated autopsies was exempted by the NYU Grossman School of Medicine Institutional Review Board. Consent was provided by the legal next of kin in each case.

3. Results

Table 1 summarizes the clinical presentation of the cases. The age range was 44–65 years, and four of seven cases were female. Two presented with asystolic arrest at home after reporting symptoms for several days. Two patients were known to be taking aspirin before they became ill. None were taking anticoagulation before illness, but the five patients who survived to hospitalization all received either therapeutic or prophylactic anticoagulation. Each of the five hospitalized patients received at least one dose of azithromycin and hydroxychloroquine, and some received IL-1 and IL-6 inhibitors (Table 1). All hospitalized patients were mechanically ventilated. All patients who died in hospital had pulseless electrical activity (PEA). The two patients who died at home had asystole at first medical contact.

Table 1
Clinical and Key Laboratory Information for Cases 1–7.

Patient Characteristics	Case 1	Case 2	Case 3	Case 4	Case 5	Case 6	Case 7
Age – yr, Sex	64, Female	60, Male	50, Female	44, Male	64, Female	55, Female	65, Male
Race/Ethnicity	White	White	Hispanic	Black	Hispanic	Hispanic	White
Symptoms before hospitalization	3d dyspnea and flu-like illness	7d fever, chills, dyspnea	7d fever, cough, dyspnea	7d fever, cough, myalgia	7d fever, cough, dyspnea	14d fever, cough, dyspnea, malaise	14d dyspnea and cough
Hospitalization to death – days	0	0	2	6	9	11	3
Symptom onset to death – days	3	7	9	13	16	25	17
Cardiac arrest details	Asystolic arrest at home	Asystolic arrest at home	PEA arrest	PEA arrest	PEA arrest, no CPR	PEA arrest, no CPR	PEA arrest, no CPR
Hypertension	Yes	Yes	Yes	Yes	Yes	No	Yes
High cholesterol	Yes	No	Yes	Yes	Yes	No	No
Diabetes	Yes	Yes	Yes	Yes	No	No	Yes
Obesity	Yes	Yes	No	Yes	Yes	Yes	No
BMI – kg/m^2	36⍰0	32⍰3	23⍰0	38⍰8	35⍰6	30⍰7	25⍰0
Other Key Medical History	COPD, lung cancer	Coronary artery disease	N/A	Renal cell carcinoma	Obstructive sleep apnea	N/A	Cirrhosis, PAD, CKD, hypothyroidism
Outpatient antiplatelet/ anticoagulation	Aspirin	Unknown	None	None	Aspirin	None	None
Inpatient Anticoagulation/Antiplatelet	N/A	N/A	Enoxaparin 40 mg daily	Unfractionated heparin drip	Aspirin and unfractionated heparin drip transitioned to enoxaparin 1 mg/kg q12h	Enoxaparin 40 mg daily, transitioned to unfractionated heparin drip, then enoxaparin 1 mg/kg q12h	Unfractionated heparin drip, stopped <2 h after admission
Other Relevant Inpatient Rx	N/A	N/A	Azithromycin, HCQ	Azithromycin, HCQ	Azithromycin, HCQ, tocilizumab, anakinra	Azithromycin, HCQ, tocilizumab	Azithromycin, HCQ, tocilizumab
Peak D-dimer, ng/mL	N/A	N/A	N/A	320	10,287	5483	>52,926
Peak troponin, ng/mL	N/A	N/A	0⍰4	0⍰8	11⍰0	<0⍰1	34⍰8

All patients were positive for SARS-CoV-2 using the GeneExpert (Cepheid) test and negative for other respiratory viral pathogens on the Cepheid analyzer, including common coronaviruses, before and/or after death.
Figure Legends.

Additional details of the laboratory findings, imaging findings, and hospital courses are in Supplemental Tables 1–2.

3.1. Multi-organ thrombosis and megakaryocytes

All cases, regardless of anticoagulation received, demonstrated platelet-rich thrombi in the pulmonary, hepatic, renal, and cardiac microvasculature (Fig. 1). In the lungs, thrombi involved large and small vessels, and platelets were noted within the alveolar capillaries. There were pulmonary arterial thrombi in four cases, three of which had received anticoagulation (two at therapeutic dose and one at prophylactic dose). This included obstructive, predominately white thrombus in the right main pulmonary artery, and multiple right ventricular mural thrombi, in case 4, and segmental pulmonary artery thrombi in cases 3, 4 (bilateral) and 7 (Fig. 2). Pulmonary artery casts conformed to the anatomic location in which they were found. The presence of lines of Zahn in pulmonary, and cardiac intravascular thrombi strongly suggests antemortem thrombosis. Thrombi were not found in the inferior vena cava. However, the deep leg veins were not dissected.

Megakaryocytes were seen in all cases in the microvasculature of the heart, in some glomeruli, and in higher than usual numbers in the lungs (Fig. 3, Supplemental Fig. 1). The median number of megakaryocytes/HPF in lung was 9 (interquartile range [IQR], 4–19) in COVID-19 and 3 (IQR 2–5) in other ARDS, $p = 0{\cdot}01$. The number of megakaryocytes in bone marrow was increased with focal clustering. Bone marrow megakaryocyte morphology suggested active platelet production, with prominent pseudopodia. Megakaryocyte numbers were increased in COVID-19 hearts as compared with other ARDS (median 4.5, IQR 3–8, in COVID-19 vs. median 1, IQR 0–3, in ARDS, $p = 0{\cdot}02$). Rare virions were identified on electron microscopy in bone marrow megakaryocytes (Supplemental Fig. 2).

3.2. Cardiac findings

In all cases, megakaryocytes associated with fibrin microthrombi were identified within the cardiac microvasculature. There were no viral inclusions on electron microscopy of the heart in any of four cases analyzed (cases 2, 4, 6 and 7). Only one patient (case 4) exhibited a focal inflammatory infiltrate composed of lymphocytes, mixture of B and T cells as per CD20 and CD3, with CD4 in greater number than CD8, with associated myocardial necrosis in the epimyocardial region (Fig. 4). Despite thorough sectioning, the infiltrate was localized, even though there was diffuse, transmural pallor of the left ventricle. Immunohistochemical staining for CD61 (platelet glycoprotein IIIa), a megakaryocytic and platelet marker, identified platelet microthrombi in the region of inflammation. There were no electrocardiographic abnormalities on admission or on the day of death in this patient, nor were there granulomas. Staining for complement (C4d) was performed to rule out complement-mediated myocyte damage and was negative in all cases tested.

Venous thrombosis was identified in two hearts (cases 3 and 7). In case 7, there was intramyocardial venous thrombosis with septal myocardial infarction (MI) despite only minimal coronary atherosclerosis (Fig. 5). This patient also had cirrhosis of the liver due to alcohol, and there were elevated levels of antiphospholipid IgM antibodies detected post-mortem. The peak troponin was 34·8 ng/mL, measured on the day of death (hospitalization day three). A limited cardiac ultrasound performed three hours after troponin showed right ventricular hypokinesis. Left ventricular wall motion was normal on this limited study with only subcostal views. The electrocardiogram (ECG) at admission showed hyperacute T waves in V2, and ECG on the day of death showed inferolateral ST elevations with hyperacute T waves in leads V2-V3. In case 3, there was epicardial venous thrombosis, but MI was not noted on gross nor microscopic inspection

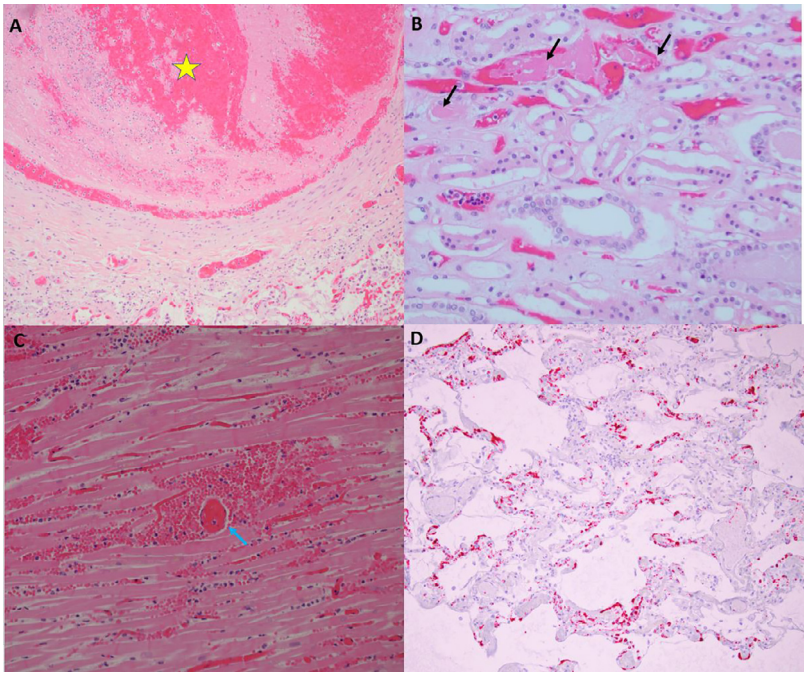

Fig. 1. Thrombosis in multiple organs at autopsy. Panel A, Case 3, 20x magnification of hematoxylin and eosin stained section, medium vessel pulmonary artery thrombus (yellow star) with lines of Zahn and fibrin thrombus without organization in a smaller arteriole (yellow arrow). The adjacent lung shows similar temporal relationship with exudative phase of diffuse alveolar damage with hyaline membrane formation. Panel B, Case 2, 20x magnification of hematoxylin and eosin stained section of medulla of the kidney with fibrin microthrombi in the peritubular capillaries (black arrows). The tubular epithelium shows detachment from the basement membrane with vacuolization as well as granular debris within the tubular lumen. Panel C, Case 7, 20x magnification of hematoxylin and eosin stained section. Cardiac tissue with fibrin thrombus in a perforating vein (blue arrow) associated with a myocardial infarction showing myocardial necrosis, which was transmural, and neutrophilic infiltrates. Panel D, Case 2, 10x magnification of hematoxylin and eosin stained section. Platelet microthrombi highlighted by CD61 immunohistochemical stain within the microvasculature of the lung. (For interpretation of the references to color in this figure legend, the reader is referred to the web version of this article.)

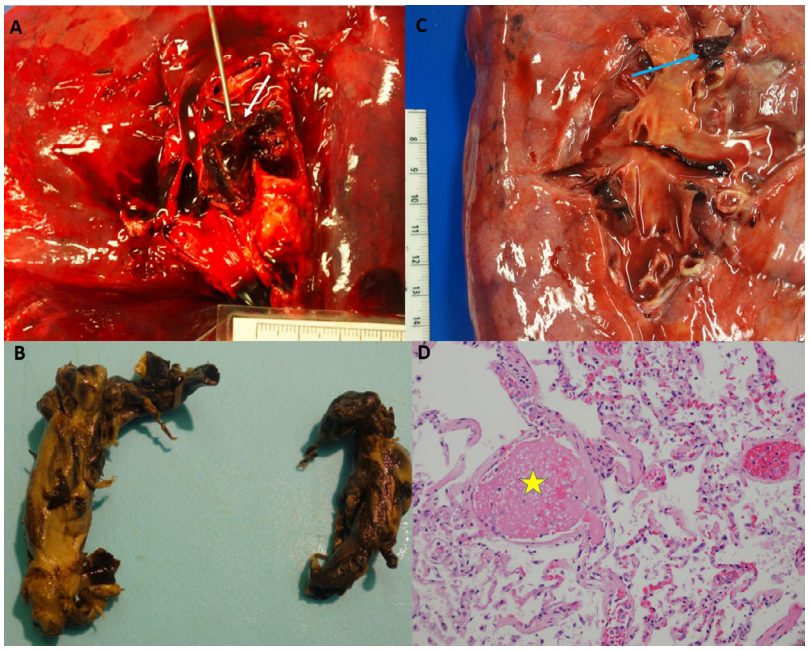

Fig. 2. Pulmonary thrombi. Panel A: Case 4, Large occlusive pulmonary thrombus within the right main pulmonary artery (white arrow). Panel B: Case 4, Thrombus easily removed showing a predominately white thrombus that is molded in the anatomic pattern of the pulmonary vasculature. Panel C: Case 5, Loosely adherent pulmonary thrombus within a segmental pulmonary artery of the left lung (blue arrow). Panel D: Case 5, H&E 40x, microscopic image of the lung showing changes of diffuse alveolar damage as well as a fibrin microthrombus (yellow star). (For interpretation of the references to color in this figure legend, the reader is referred to the web version of this article.)

(Supplemental Fig. 3). Troponin, measured four hours before death, was 0·4 ng/dL, within the normal limits at our laboratory.

Otherwise, cardiac histopathological changes were limited to minimal epicardial inflammation ($n = 1$), early ischemic injury ($n = 3$), and mural fibrin thrombi ($n = 2$).

3.3. *Lung parenchyma*

There was congestion on gross examination in all cases (representative images, Supplemental Fig. 4). All cases exhibited diffuse alveolar damage (DAD) with hyaline membrane formation, type II pneumocyte desquamation, with a mixture of exudative, and proliferative phases of DAD, corresponding to ARDS. Rare virions were identified by immunohistochemical staining for nuclear capsid protein and by electron microscopy (Supplemental Fig. 5). Granulomas were not observed. Immunostains with CD61 revealed platelet-rich thrombi in the pulmonary microvasculature. In case one there was a sparse septal and perivascular lymphocytic infiltrate, predominantly composed of CD3 positive T cells with a predominance of CD4 positive cells over CD8 positive cells. Three cases had superimposed acute bronchopneumonia, focally necrotizing, one of which had an erosive bronchitis with fungal hyphae detected.

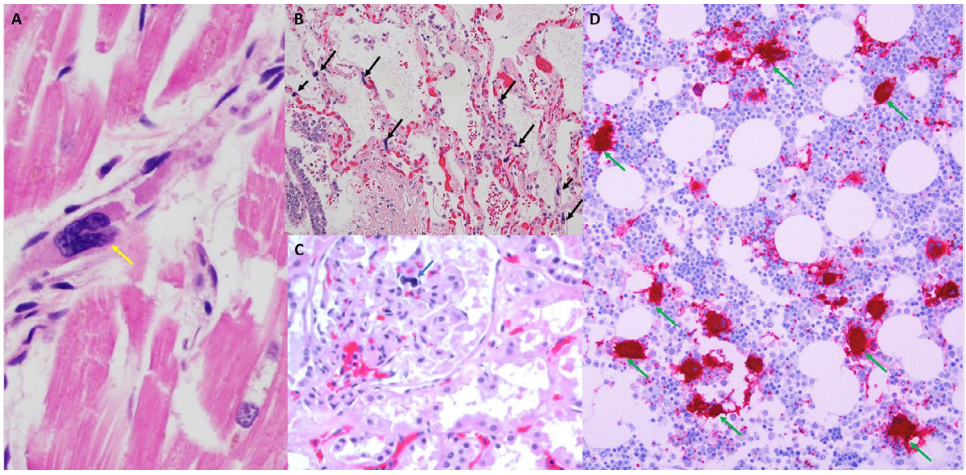

Fig. 3. Megakaryocytes in the heart, kidney, lung and bone marrow. Panel A: Case 4, 40x H&E stain, Heart with early ischemic changes and megakaryocyte (yellow arrow) and fibrin thrombus within the lumen of a venule. Panel B: Case 2, 20x H&E stain, Lung with pulmonary edema and early bronchopneumonia with multiple megakaryocytes (black arrows) within the alveolar capillaries. Panel C: Case 4, 20x H&E stain, Megakaryocyte within the capillary loop of a glomerulus (blue arrow). Panel D: Case 3, Hypercellular marrow for age with trilineage hematopoiesis. There is an increased number of megakaryocytes with focal clustering (green arrows). Myeloid elements show only focal evidence of progressive maturation (left shift). Megakaryocytes and platelets are highlighted by CD61 staining. (For interpretation of the references to color in this figure legend, the reader is referred to the web version of this article.)

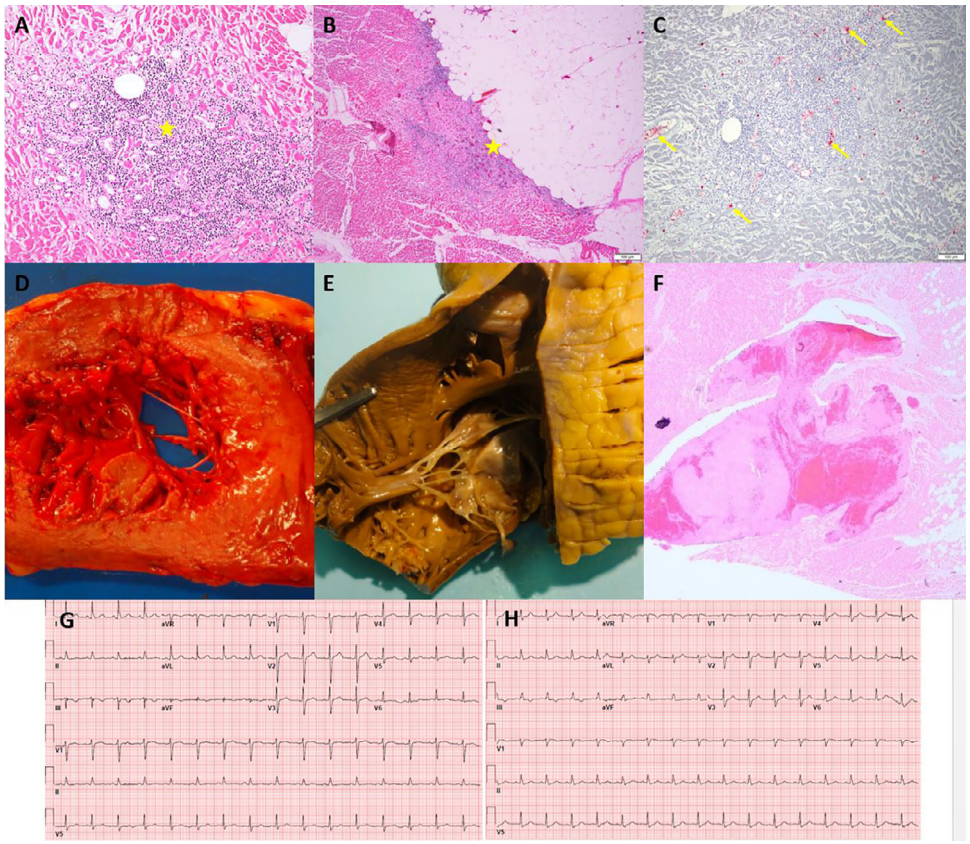

Fig. 4. Myocardial Inflammation and Right Ventricular Mural Thrombus (Case 4). Panels A and B: H&E 10x, Myocardium with a focal chronic inflammatory infiltrate composed of lymphocytes with associated myocardial necrosis in the epicardial region (yellow stars). Panel C: Platelet microthrombi highlighted by CD61 immunohistochemical stain within the microvasculature of the heart (yellow arrows), 10x. Panel D: Gross image of a cut section of the heart showing transmural diffuse pallor of the left ventricle. Panel E: Right ventricle of the heart with mural white thrombus within the trabeculae carnae. Panel F: Microscopic findings in the right ventricle of the heart with mural white thrombus within the trabeculae carnae. Panel G: Admission ECG shows normal sinus rhythm without significant ST segment abnormality.

3.4. Kidneys

Platelet-rich fibrin microthrombi were seen in scattered peritubular capillaries and venules (Fig. 1). Despite some autolysis, acute tubular necrosis, cellular casts, and some pigmented red blood cell casts were seen in all cases (Fig. 3). Thrombotic microangiopathy within the glomeruli with large platelet-rich microthrombi, red cell fragmentation and mesangiolysis was seen in case 7, but not in other cases, where only rare small glomerular platelet aggregates were seen. Several patients exhibited microhemorrhages within the interstitium, and rare schistocytes were observed. All of the cases exhibited mild to moderate arteriolosclerosis, and one demonstrated arteriolar hyalinosis, Electron microscopy showed virions in proximal convoluted tubules, and rare podocyte virions (Supplemental Fig. 5). No changes to glomerular vessels, foot processes or glomerular basement membrane were observed on light or electron microscopy. Stains for immunoglobulin, and complement were negative in cases 1 and 2.

3.5. Hematopoietic tissues

Bone marrow was hypercellular with increased megakaryocytes demonstrating focal clustering. There was progressive maturation of myeloid series with left shift and reduced erythropoiesis. Hemophagocytosis was not identified. Red blood cells with abnormal morphology resembling burr cells (echinocytes) were commonly seen. Spleens were congested, partially autolyzed in one case. In most cases, there was white pulp depletion, congestion of the red pulp, and no evidence of extramedullary hematopoiesis. Similar to what was observed in the lung, there was a predominance of T cells with slight CD4 excess. Lymph nodes analyzed from 5 cases showed dilated sinuses with marked sinus histiocytosis with focal erythrophagocytosis, numerous platelets, and megakaryocytes (best appreciated by CD61 stain). Secondary follicles in the far cortex appeared hypocellular. Lymph nodes were not readily located in the remaining cases or were grossly unremarkable.

3.6. Liver

All of the cases showed mild, macrovesicular steatosis without significant inflammation or ballooning suggestive of steatohepatitis. Case 7 showed cirrhosis. Numerous platelet-fibrin microthrombi were identified in hepatic sinusoids (Supplemental Fig. 6) in six cases, but case 1 showed only rare microthrombi. Ischemic type hepatic necrosis was associated with the microthrombi in two of seven cases (3 and 5). Larger platelet aggregates were also noted in the portal veins in these two cases. In case 5, this was associated with zone 3 necrosis with a hepatic vein thrombus.

3.7. Adipose tissue

Epicardial, and mesenteric adipocytes were of variable size with evidence of lysis. A scattered lymphocytic infiltrate was present.

4. Discussion

In this series of seven autopsies in patients who succumbed to COVID-19, there are several unifying themes observed in the

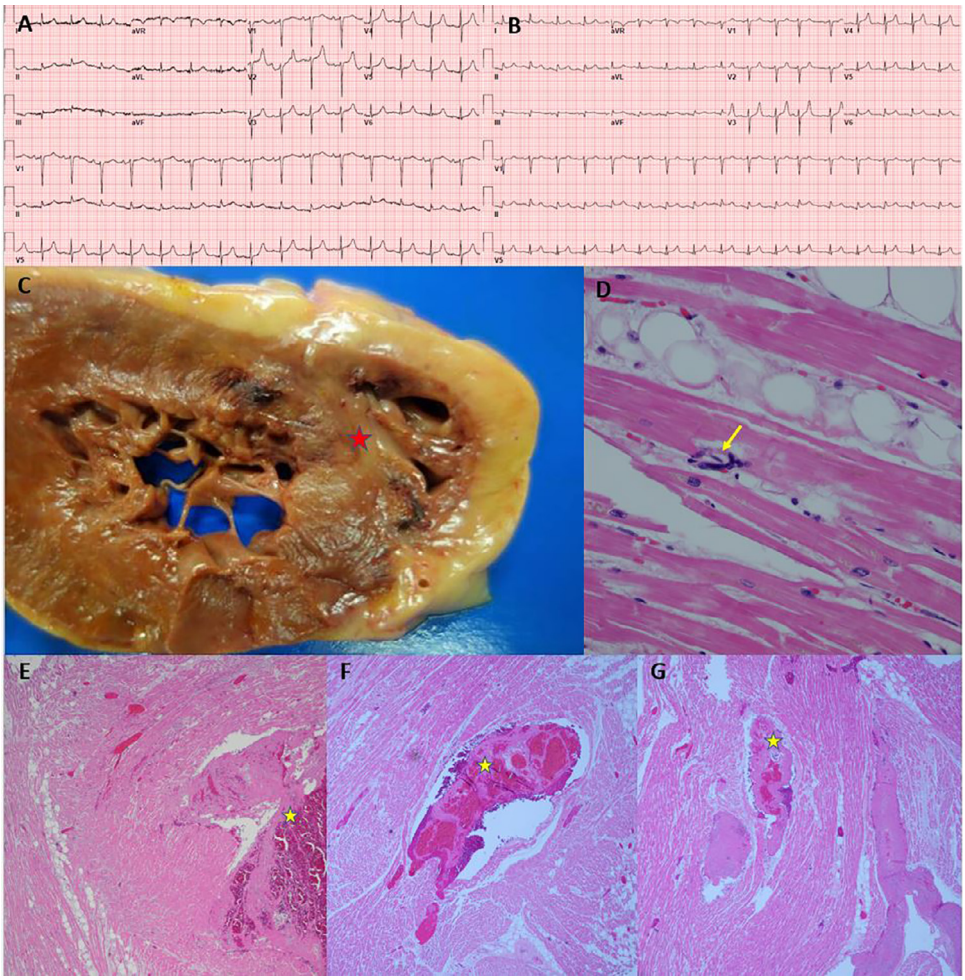

Fig. 5. Myocardial Infarction due to Venous Thrombosis (Case 7). Panel A: Admission ECG showing normal sinus rhythm. Panel B: ECG after intubation (day of death), showing sinus rhythm with premature atrial contraction and inferolateral ST segment elevation. Panel C: Cut section of left and right ventricle showing pallor with peripheral hemorrhage rim at the juncture of the posterior ventricles and interventricular septum (red star). Panel D: Microscopic section showing megakaryocyte within a small vessel in the myocardium (yellow arrow). Panels E, F, G: H&E sections of the right and left ventricle with intramyocardial venous thrombosis (yellow stars), fibrin microthrombi and varying degrees of infarction.

histopathology. Thrombosis is a prominent feature in multiple organs, in some cases despite full anticoagulation. Platelet-rich thrombi were present in the pulmonary, hepatic, renal, and cardiac microvasculature. Based on the anatomic cast pattern of the thrombi, many of the thrombi appear to have formed in situ and ante-mortem, evidenced by lines of Zahn. However, embolism with further local propagation cannot be excluded based on the lack of deep vein dissection.

The extensive nature of platelet-fibrin thrombi in the alveolar capillaries in our patients may explain the observation that oxygenation is disrupted in an exaggerated fashion early in the disease course of patients with COVID-19, [16] as this suggests evidence of ventilation-perfusion mismatch unrelated to hyaline membrane formation. Our patients' lungs all had histopathologic findings of DAD, which has been the most frequently reported finding in COVID-19 autopsies thus far [10-12,17].

Our findings highlight a potential significant role of megakaryocytes and platelets in diffuse microvascular thrombosis in COVID-19. Megakaryocytes were found in the microvasculature of the heart in all cases, in glomeruli, and in increased numbers in the lungs. Bone marrow megakaryocytes were mildly increased in number with morphologic features indicating active platelet production, and contained virions as identified on electron microscopy (Supplemental Figure 2). These findings, in conjunction with extensive platelet-fibrin microthrombi detected on specific staining, suggest a profound platelet response in COVID-19 that may be responsible at least in part for multi-organ failure. The conspicuous finding of megakaryocytes along with platelet-fibrin microthrombi within the heart microvasculature in this subset of gravely ill patients with COVID-19 is provocative. There are rare reports of megakaryocytes within the heart; in the largest published series, there was an average of 1−1.9 intravascular megakaryocytes in one cm^2 of heart from 190 autopsies, involving traumatic and in-hospital deaths [18,19]. Notably, 49 of 190 cases were labeled as "infection and thrombosis." Circulating megakaryocytes have been observed in MI, another thrombotic disorder [20]. In our experience, and supported by these studies, it is rare to find megakaryocytes within the heart. Our finding of platelet microthrombi in association with megakaryocytes in the microvasculature may provide a window into mechanisms of disease in patients with fatal COVID-19.

Thrombi were located in veins and in the pulmonary arteries and arterioles and in microvessels, but not in systemic arteries. Despite elevated fibrin degradation products, in only one case of a patient with cirrhosis did we observe glomerular thrombotic microangiopathy, arguing against disseminated intravascular coagulation, hemolytic-uremic syndrome, or thrombotic thrombocytopenic purpura as a predominant pathophysiological pathway [21]. Schistocytes may suggest endothelial damage, but we found them only rarely. We found no endothelial abnormalities on microscopic review, in alignment with previous studies, but we cannot rule out increased exposure of tissue factor, erosion of the endothelial glycocalyx, or other

mechanisms of endothelial dysfunction that could be pro-coagulant without showing histopathologic evidence of cell activation or erosion [13,22,23]. A recent autopsy series of COVID-19 cases incorporating endothelial electron microscopy demonstrated ultrastructural endothelial damage and increased angiogenesis as compared to cases of fatal influenza, with differential regulation of genes related to angiogenesis and inflammation [24].

Four of the seven patients in this series had pulmonary arterial thrombi. There are now multiple autopsy reports demonstrating a high prevalence of pulmonary arterial thrombi in the setting of COVID-19 infection, including symptomatic thrombi and thrombi in the absence of coexisting deep venous thrombosis [6,7,10-12,22,25]. Each of the thrombus casts in our patients conformed to the walls of pulmonary vasculature. This appearance suggests that the thrombi were formed in situ in pulmonary arteries rather than as the result of embolization, a conclusion also reached in prior reports [6,7,10]. However, it remains possible that the large thrombi progressed rapidly, originating from smaller emboli without time for development of organization and adherence to the vessel wall. Case 6 had normal lower extremity venous duplex. However, our autopsies did not include dissection of the extremities to evaluate for deep vein thrombosis based on infection control restrictions. All patients tested had abnormal PT/INR and D-dimer.

Troponin elevation is common in COVID-19 patients and is associated with increased risk of death [2-4]. It may be surprising then that there was little myocardial inflammatory infiltrate in this case series, particularly considering that the heart expresses ACE2, a membrane protein used by SARS-CoV-2 as an attachment receptor. Only one patient (case 4) had a focal acute lymphocytic epimyocarditis, with no virions in cardiomyocytes. This mild epicardial inflammation did not cause any ST-segment deviation on ECG. The patient had minimally elevated troponin on the day of death, but the point of care ultrasound noted reduced ejection fraction. The single focus of mild epicardial inflammation in this patient may be nonspecific. Multiple additional sections of cardiac tissue were taken without further evidence of inflammation. One would expect more inflammation if cardiomyopathy were due to fulminant lymphocytic myocarditis. Here, cardiomyopathy may be attributable to profound metabolic derangements, with severe metabolic and respiratory acidosis at the time of the cardiac ultrasound, immediately preceding cardiac arrest.

Though troponin elevation in patients with COVID-19 has often been ascribed to myocarditis by clinicians, there have been very few reports of myocarditis with accompanying tissue samples showing lymphocytic infiltrate [22,25–28]. One of the three previously published autopsy reports showing myocarditis described a COVID-19 patient who was co-infected with influenza [26]. When present, the infiltrate may be focal and epicardial, as seen in our one case with myocardial inflammation [22,27]. Thus tissue-proven viral myocarditis appears to be relatively rare in COVID-19, and other mechanisms of myocardial injury must be considered. No evidence of complement-mediated myocardial damage was present in our cohort, though we and others have demonstrated this previously in the setting of influenza [29,30]. Another group reported a high degree of complement deposition in lung, and skin in COVID-19 patients, but did not assess cardiac tissue [13]. There are many potential causes of troponin elevation including ischemia, inflammation, metabolic derangement and trauma. Right ventricular strain due to pulmonary thrombosis and hypertension is another potential mechanism [31]. Based on our data, thrombosis of the microvasculature and cardiac veins appears to be a common cause of elevated troponin in COVID-19.

We demonstrate for the first time, to our knowledge, that thrombosis of a cardiac vein can cause acute MI in the absence of obstructive coronary atherosclerosis. ST segment elevation on the ECG may prompt urgent coronary angiography in COVID-19 patients. Our group has reported that there is no obstructive coronary artery disease in approximately one-third of such cases [5]. MI with non-obstructive coronary arteries is increasingly recognized [32]. It remains to be learned whether myocardial venous thrombosis may in fact cause this entity in clinical situations other than COVID-19 illness. Case 3 had thrombosis of an intramyocardial vein corresponding to the infarction zone. While case 7 also had venous thrombosis, in the middle cardiac vein (epicardial), there was no gross or microscopic evidence of MI. A proposed explanation for this finding may be that thrombosis occurred just prior to cardiac arrest, since evidence of infarction on gross or histopathology appears hours after ischemia onset.

Renal findings in our patients shed light on the pathogenesis of acute kidney injury in COVID-19. Virions were observed in proximal tubular cells. Acute tubular necrosis and peritubular fibrin thrombi were apparent. A recently reported series of 26 autopsies in COVID-19 showed acute tubular injury of varying severity in all cases, with prominent microvascular obstruction by erythrocytes [33]. Renal tubular cells are known to present ACE2, the viral receptor, so it is logical that virions are most prominent in this location. The absence of virus in endothelial cells, rare infection of podocytes, and absence of visible glomerular pathology in most of our cases also argue against a glomerular cause of kidney injury, despite the proteinuria observed in many COVID-19 cases [34,35].

Obesity is a major risk factor for COVID-19 morbidity, and mortality, though the mechanism for this relationship is not yet clear [36]. Adipose tissue expresses ACE2. Adipocytes are a known contributor to the inflammatory cascade, upregulating cytokines such as TNF-α, IL-1, and IL-6 [37]. Inflammatory dysregulation by infected adipocytes could exacerbate inflammation thus contributing to ARDS and the prothrombotic milieu. While adipocytes have been implicated as a reservoir for organisms like HIV, Trypanosoma cruzi, and influenza A, there is currently no evidence to suggest that obesity is correlated with SARS-COV-2 viral clearance [38,39]. Dipeptidyl peptidase 4 (DPP-4) is highly expressed on adipocytes and may play a role in COVID-19 infection, as it was implicated as a functional receptor for the spike protein of the Middle East Respiratory Syndrome-related coronavirus [40]. In addition to its role in insulin metabolism, DPP-4 contributes to systemic inflammation and immune regulation via pathways including T cell activation [41].

Erythrophagocytosis was observed in lymph nodes. This nonspecific finding can be seen in multiple severe inflammatory conditions, including sepsis, macrophage activating syndrome and hemophagocytic lymphohistiocytosis [42]. The significance of echinocytes in these cases is unclear, and here may be most related to abnormal pH.

Our study has several limitations. The sample size is limited and was based on referral for autopsy rather than pre-specified clinical parameters. Laboratory testing was performed according to clinical routine and not done systematically; we do not have results for all laboratory parameters of interest in all cases. Brain and deep leg veins were not evaluated based on autopsy restrictions for infection control. Electron microscopy was performed on a limited basis due to limited availability of resources during the pandemic, and infection control concerns.

In this series of seven COVID-19 autopsies, macrovascular and microvascular thrombosis was a prominent feature, in some cases despite full anticoagulation. There were platelet-rich microthrombi and circulating megakaryocytes in multiple organs. One case demonstrated acute myocardial infarction due to thrombosis in intramural coronary veins, and one case had focal myocarditis. Despite elevated fibrin degradation products, findings typical of renal thrombotic microangiopathy in glomeruli were absent in all but one case, arguing against classical disseminated intravascular coagulation as the underlying pathophysiologic mechanism.

Funding

There was no external funding for this analysis. This study was supported, in part, by the Intramural Research Program of the NIH, National Cancer Institute.

Declaration of Competing Interest

Dr. Rapkiewicz, Dr. Mai, Dr. Pittaluga, Dr. Thomas, Dr. Kleiner, Dr. Adler and Dr. Gasmi have nothing to disclose.

Dr. Carsons reports grants from Novartis and grants from GSK, outside the submitted work.

Dr. Berger reports grants from National Heart, Lung and Blood Institute, during the conduct of the study; grants from Astrazeneca, other from Jannsen, other from Amgen, outside the submitted work.

Dr. Charytan reports personal fees from PLC Medical, grants from bioporto, personal fees from Merck, grants and personal fees from NovoNordisk, grants and personal fees from Jannssen, grants and personal fees from Gilead, personal fees from AstraZeneca, grants and personal fees from Medtronic, grants and personal fees from Amgen, personal fees from Fresenius, personal fees from GSK, outside the submitted work.

Dr. Hochman was supported in part by the NYU CTSA grant UL1TR001445, from the National Center for Advancing Translational Sciences (NCATS) during the conduct of the study; grants from NHLBI, other from AstraZeneca Pharmaceuticals LLC, other from Arbor Pharmaceuticals LLC, non-financial support from Abbott Vascular, non-financial support from Medtronic Inc, non-financial support from St. Jude Medical Inc, non-financial support from Volcano Corp, non-financial support from Merck Sharp & Dohme Corp, non-financial support from Omron Healthcare Inc, non-financial support from Amgen Inc, outside the submitted work.

Dr. Reynolds reports non-financial support from Abbott Vascular, non-financial support from Siemens, non-financial support from Biotelemetry Inc outside the submitted work.

Acknowledgments

The authors thank NYU Langone Health DART Microscopy Lab Alice Liang, and Kristen Dancel-Manning, NYU Winthrop electron microscopist Thomas Palaia and Julie Alejo at the Center for Cancer Research at NCI for their assistance with electron microscopy. The NYU Langone Health DART Microscopy Laboratory is partially funded by NYU Cancer Center Support Grant NIH/NCI P30CA016087.

Supplementary materials

Supplementary material associated with this article can be found in the online version at doi:10.1016/j.eclinm.2020.100434.

References

[1] Wang D, Hu B, Hu C, et al. Clinical characteristics of 138 hospitalized patients with 2019 novel coronavirus-infected pneumonia in Wuhan, China. JAMA 2020;323 (11):1061–9.
[2] Chen T, Wu D, Chen H, et al. Clinical characteristics of 113 deceased patients with coronavirus disease 2019: retrospective study. BMJ 2020;368:m1091.
[3] Guo T, Fan Y, Chen M, et al. Cardiovascular Implications of Fatal Outcomes of Patients With Coronavirus Disease 2019 (COVID-19). JAMA Cardiol 2020:e201017.
[4] Shi S, Qin M, Shen B, et al. Association of Cardiac Injury With Mortality in Hospitalized Patients With COVID-19 in Wuhan, China. JAMA Cardiol 2020 Published online March 25, 2020.
[5] Bangalore S, Sharma A, Slotwiner A, et al. ST-Segment Elevation in Patients with Covid-19 - A Case Series. N Engl J Med 2020 NEJMc2009020.
[6] Poissy J, Goutay J, Caplan M, et al. Pulmonary Embolism in COVID-19 Patients: awareness of an Increased Prevalence. Circulation 2020.
[7] Middeldorp S, Coppens M, van Haaps TF, et al. Incidence of venous thromboembolism in hospitalized patients with COVID-19. J Thromb Haemost 2020. doi: 10.1111/jth.14888.
[8] Klok FA, Kruip M, van der Meer NJM, et al. Incidence of thrombotic complications in critically ill ICU patients with COVID-19. Thromb Res 2020;191:145–7.
[9] Bikdeli B, Madhavan MV, Jimenez D, et al. COVID-19 and thrombotic or thromboembolic disease: implications for prevention, antithrombotic therapy, and follow-up. J Am Coll Cardiol 2020;75(23):2950–73.
[10] Lax SF, Skok K, Zechner P, et al. Pulmonary arterial thrombosis in COVID-19 with fatal outcome: results from a prospective, single-center, clinicopathologic case series. Ann Intern Med 2020 M20–2566.
[11] Menter T, Haslbauer JD, Nienhold R, et al. Post-mortem examination of COVID19 patients reveals diffuse alveolar damage with severe capillary congestion and variegated findings of lungs and other organs suggesting vascular dysfunction. Histopathology 2020. doi: 10.1111/his.14134.
[12] Wichmann D, Sperhake JP, Lutgehetmann M, et al. Autopsy findings and venous thromboembolism in patients With COVID-19. Ann Intern Med 2020 May 6 M20–2003.
[13] Magro C, Mulvey JJ, Berlin D, et al. Complement associated microvascular injury and thrombosis in the pathogenesis of severe COVID-19 infection: a report of five cases. Transl Res 2020;220:1–13.
[14] Paranjpe I, Fuster V, Lala A, et al. Association of Treatment Dose Anticoagulation with In-Hospital Survival Among Hospitalized Patients with COVID-19. J Am Coll Cardiol 2020;S0735-1097(20) 35218–9.
[15] Tang N, Bai H, Chen X, Gong J, Li D, Sun Z. Anticoagulant treatment is associated with decreased mortality in severe coronavirus disease 2019 patients with coagulopathy. J Thromb Haemost 2020;18:1094–9.
[16] Gattinoni L, Coppola S, Cressoni M, Busana M, Rossi S, Chiumello D. COVID-19 does not lead to a "Typical" acute respiratory distress syndrome. Am J Respir Crit Care Med 2020;201:1299–300.
[17] Barton LM, Duval EJ, Stroberg E, Ghosh S, Mukhopadhyay S. COVID-19 autopsies, Oklahoma, USA. Am J Clin Pathol 2020;153:725–33.
[18] Brill R, Halpern MM. The frequency of megakaryocytes in autopsy sections. Blood 1948;3:286–91.
[19] Smith EB, Butcher J. The incidence, distribution and significance of Megakaryocytes in normal and diseased human tissues. Blood 1952;7:214–24.
[20] Van Pampus EC, Huijgens PC, Zevenbergen A, Verheugt FW, Langenhuijsen MM. Circulating human megakaryocytes in cardiac diseases. Eur J Clin Invest 1994;24:345–9.
[21] Brocklebank V, Wood KM, Kavanagh D. Thrombotic Microangiopathy and the Kidney. Clin J Am Soc Nephrol 2018;13:300–17.
[22] Edler C, Schroder AS, Aepfelbacher M, et al. Dying with SARS-CoV-2 infection-an autopsy study of the first consecutive 80 cases in Hamburg, Germany. Int J Legal Med 2020:1–10.
[23] Varga Z, Flammer AJ, Steiger P, et al. Endothelial cell infection and endotheliitis in COVID-19. Lancet 2020;395:1417–8.
[24] Ackermann M, Verleden SE, Kuehnel M, et al. Pulmonary Vascular Endothelialitis, Thrombosis, and Angiogenesis in Covid-19. N Engl J Med 2020. doi: 10.1056/NEJMoa2015432.
[25] Fox SE, Akmatbekov A, Harbert JL, Li G, Quincy Brown J, Vander Heide RS. Pulmonary and cardiac pathology in African American patients with COVID-19: an autopsy series from New Orleans. Lancet Respir Med 2020;S2213-2600(20) 30243–5.
[26] Bradley BT, Maioli H, Johnston R, et al. Histopathology and ultrastructural findings of fatal COVID-19 infections. medRxiv 2020 2020.04.17.20058545.
[27] Buja LM, Wolf DA, Zhao B, et al. The emerging spectrum of cardiopulmonary pathology of the coronavirus disease 2019 (COVID-19): report of 3 autopsies from Houston, Texas, and review of autopsy findings from other United States cities. Cardiovasc Pathol 2020;48:107233.
[28] Sala S, Peretto G, Gramegna M, et al. Acute myocarditis presenting as a reverse Tako-Tsubo syndrome in a patient with SARS-CoV-2 respiratory infection. Eur Heart J 2020;41:1861–2.
[29] Paddock CD, Liu L, Denison AM, et al. Myocardial injury and bacterial pneumonia contribute to the pathogenesis of fatal influenza B virus infection. J Infect Dis 2012;205:895–905.
[30] Siskin M, Rao S, Rapkiewicz A, Bangalore S, Garshick M. A Case of Cardiogenic Shock Secondary to Complement-Mediated Myopericarditis From Influenza B Infection. Can J Cardiol 2017;33 1335 e1- e3.
[31] Szekely Y, Lichter Y, Taieb P, et al. The Spectrum of Cardiac Manifestations in Coronavirus Disease 2019 (COVID-19) - a Systematic Echocardiographic Study. Circulation 2020;2020. doi: 10.1161/CIRCULATIONAHA.120.047971.
[32] Tamis-Holland JE, Jneid H, Reynolds HR, et al. Contemporary diagnosis and management of patients with myocardial infarction in the absence of obstructive coronary artery disease: a scientific statement from the American Heart Association. Circulation 2019;139:e891–908.
[33] Su H, Yang M, Wan C, et al. Renal histopathological analysis of 26 postmortem findings of patients with COVID-19 in China. Kidney Int 2020;S0085-2538(20) 30369–0.
[34] Cheng Y, Luo R, Wang K, et al. Kidney disease is associated with in-hospital death of patients with COVID-19. Kidney Int 2020;97:829–38.
[35] Li Z., Wu M., Yao J., et al. Caution on Kidney Dysfunctions of COVID-19 Patients. medRxiv2020:2020.02.08.20021212.
[36] Goyal P, Choi JJ, Pinheiro LC, et al. Clinical Characteristics of Covid-19 in New York City. N Engl J Med 2020;382(24):2372–4.
[37] Kern L, Mittenbuhler MJ, Vesting AJ, Ostermann AL, Wunderlich CM, Wunderlich FT. Obesity-induced TNFalpha and IL-6 signaling: the missing link between obesity and inflammation-driven liver and colorectal cancers. Cancers (Basel) 2018;11.
[38] Desruisseaux MS, Nagajyothi Trujillo ME, Tanowitz HB, Scherer PE. Adipocyte, adipose tissue, and infectious disease. Infect Immun 2007;75:1066–78.
[39] Maier HE, Lopez R, Sanchez N, et al. Obesity increases the duration of influenza a virus shedding in adults. J Infect Dis 2018;218:1378–82.
[40] Raj VS, Mou H, Smits SL, et al. Dipeptidyl peptidase 4 is a functional receptor for the emerging human coronavirus-EMC. Nature 2013;495:251–4.
[41] Reinhold D, Kahne T, Steinbrecher A, et al. The role of dipeptidyl peptidase IV (DP IV) enzymatic activity in T cell activation and autoimmunity. Biol Chem 2002;383:1133–8.
[42] Simon DW, Carcillo JA. Practice Point 22 - infection-related hemophagocytic syndromes. Cohen J, Powderly WG, Opal SM, editors. Practice Point 22 - infection-related hemophagocytic syndromes. Infect Dis (Fourth Edition): Elsevier 2017;638-9:e1.